

Isotopic and Geochemical Tracers for U(VI) Reduction and U Mobility at an in Situ Recovery U Mine

Anirban Basu,^{*,†} Shaun T. Brown,^{†,‡} John N. Christensen,[‡] Donald J. DePaolo,^{†,‡} Paul W. Reimus,[§] Jeffrey M. Heikoop,[§] Giday Woldegabriel,[§] Ardyth M. Simmons,[§] Brian M. House,^{§,||} Matt Hartmann,[⊥] and Kate Maher[#]

[†]Department of Earth and Planetary Science, University of California, Berkeley, 307 McCone Hall, Berkeley, California 94720, United States

[‡]Lawrence Berkeley National Laboratory, 1 Cyclotron Road, Berkeley, California 94720, United States

[§]Earth and Environmental Sciences Division, Los Alamos National Laboratory, Los Alamos, New Mexico 87545, United States

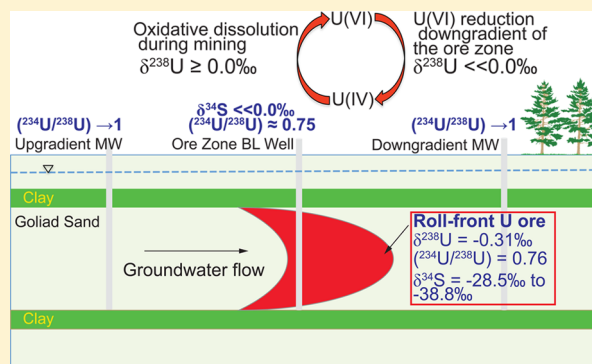
^{||}Scripps Institution of Oceanography, University of California, San Diego, La Jolla, California 92093, United States

[⊥]Uranium Resources, Inc., 6950 S. Potomac Street, Suite 300, Centennial, Colorado 80112, United States

[#]Department of Geological and Environmental Sciences, Stanford University, Stanford, California 94305, United States

Supporting Information

ABSTRACT: In situ recovery (ISR) uranium (U) mining mobilizes U in its oxidized hexavalent form (U(VI)) by oxidative dissolution of U from the roll-front U deposits. Postmining natural attenuation of residual U(VI) at ISR mines is a potential remediation strategy. Detection and monitoring of naturally occurring reducing subsurface environments are important for successful implementation of this remediation scheme. We used the isotopic tracers $^{238}\text{U}/^{235}\text{U}$ ($\delta^{238}\text{U}$), $^{234}\text{U}/^{238}\text{U}$ activity ratio, and $^{34}\text{S}/^{32}\text{S}$ ($\delta^{34}\text{S}$), and geochemical measurements of U ore and groundwater collected from 32 wells located within, upgradient, and downgradient of a roll-front U deposit to detect U(VI) reduction and U mobility at an ISR mining site at Rosita, TX, USA. The $\delta^{238}\text{U}$ in Rosita groundwater varies from +0.61‰ to -2.49‰, with a trend toward lower $\delta^{238}\text{U}$ in downgradient wells. The concurrent decrease in U(VI) concentration and $\delta^{238}\text{U}$ with an ϵ of 0.48‰ \pm 0.08‰ is indicative of naturally occurring reducing environments conducive to U(VI) reduction. Additionally, characteristic $^{234}\text{U}/^{238}\text{U}$ activity ratio and $\delta^{34}\text{S}$ values may also be used to trace the mobility of the ore zone groundwater after mining has ended. These results support the use of U isotope-based detection of natural attenuation of U(VI) at Rosita and other similar ISR mining sites.



INTRODUCTION

In situ recovery (ISR) of uranium (U) is a widely used subsurface mining technique by which U is extracted via oxidative dissolution of sandstone-hosted U ore deposits.^{1,2} The ISR mining approach is becoming increasingly common,³ as it enables economic recovery of low-grade ores, does not generate tailings, and has a relatively low carbon footprint.^{3–5} In 2012, ISR mining accounted for ~45% of global U production.³ In low temperature sandstone-hosted ore deposits, U primarily occurs in the tetravalent oxidation state (i.e., U(IV)) in minerals such as uraninite or coffinite.^{6,7} The mining process capitalizes on the high permeability of the ore bearing sandstone aquifer and involves injection of a lixiviant containing oxidants (e.g., dissolved oxygen, hydrogen peroxide, sulfuric acid) and complexing agents (e.g., HCO_3^-) that oxidize U(IV) to highly soluble U(VI), which forms stable uranyl carbonate complexes in the mining solution. However, ISR activity

mobilizes U as chemically toxic and bioavailable U(VI), which may potentially contaminate water resources downgradient of ISR mines when advected by groundwater after mining ceases.

Redox dependent solubility of U controls the mobility of U in the subsurface and influences a major part of low-temperature U cycling, including the formation economic U deposits. For instance, sandstone-hosted U ore deposits, comprising almost 90% of all known U resources in the United States⁸ and ~25% worldwide,⁹ originate from the reduction of dissolved U(VI) to insoluble U(IV) when U-bearing groundwaters encounter reducing conditions. A subtype of sandstone-hosted U ores, crescent-shaped roll-

Received: February 8, 2015

Revised: April 23, 2015

Accepted: April 24, 2015

Published: April 24, 2015

front deposits, are formed perpendicular to the groundwater flow direction at the interface between the reduced and oxidized portions of the aquifers.^{9–12} The redox gradient from oxidizing to progressively reducing conditions is a result of abiotic reductants (e.g., Fe(II)-bearing minerals, organic matter, aqueous Fe(II) and H₂S, CH₄) and/or microbial activity.⁸ The ISR mining perturbs the prevailing redox conditions within these deposits and creates artificially oxidizing conditions. However, naturally occurring reducing environments within and downgradient of the ore deposits may induce reductive immobilization of the U(VI) generated by ISR activity during mining fluid excursions and once the natural hydrology is restored. If effective, this postmining natural attenuation of U(VI) in groundwater would provide an inexpensive remediation strategy at ISR sites.

Naturally occurring U isotopes (e.g., ²³⁸U, ²³⁵U) may serve as indicators of environments conducive to U(VI) reduction and U mobilization. Reduction of U(VI) to U(IV) induces a mass independent isotopic fractionation due to a mechanism known as the nuclear volume effect, leading to the preferential enrichment of ²³⁸U in the U(IV) products.^{13–15} Thus, U(VI) reduction results in progressively decreasing ²³⁸U/²³⁵U in the remaining aqueous U(VI). This isotopic fractionation effect was first suggested from theoretical calculations,^{14,16} and later confirmed by observations of ²³⁸U enrichment in geological samples (e.g., black shales, and roll-front deposits)^{17–21} and field scale and laboratory batch incubation experiments on U(VI) bioreduction.^{22,23} The magnitude of the isotopic fractionation is often expressed by an isotopic enrichment factor, ϵ ($\epsilon = 1000(\alpha - 1)$; $\alpha = (^{238}\text{U}/^{235}\text{U})_{\text{product}} / (^{238}\text{U}/^{235}\text{U})_{\text{reactant}}$). Nonreductive processes (e.g., adsorption, dilution) leading to U(VI) concentration decrease do not significantly affect the U isotope ratios in aqueous systems.²⁴ Therefore, ²³⁸U/²³⁵U in groundwater is an effective indicator of U(VI) reduction.

Coexisting sulfur isotopes ($\delta^{34}\text{S}$) may also be used to assess the postmining redox state of the ISR sites. The “nose” of the roll-front deposits at many sites contains abundant sulfide minerals (i.e., Mo- and Fe-sulfides).^{25–31} Oxidative dissolution of the sulfide minerals during ISR mining generates SO₄²⁻ and hence the S isotopic composition of SO₄²⁻ can be particularly useful to detect both mineral dissolution and postmining sulfate reduction in groundwater. Sulfate reduction leads to preferential accumulation of lighter S isotopes (³²S) in sulfide (i.e., reaction product) rendering the residual sulfate in groundwater enriched in heavier ³⁴S. Both abiotic and microbial sulfate reduction to sulfide induce large fractionations; the ϵ_{S} values (defined similarly as in the above equation used for U) for abiotic and microbial sulfate reduction are 22‰ and 6–46‰, respectively.^{32,33} In contrast, oxidation of sulfide minerals to sulfate induces a smaller fractionation (<5‰) where the aqueous sulfate progressively acquires the isotopic signature of the source sulfide.³² Thus, S isotope ratios in postmining groundwater can serve as a tracer for mining fluid resulting from mineral dissolution, as well as an indicator of aqueous sulfate reduction, if any.

The ²³⁴U/²³⁸U activity ratios, expressed as (²³⁴U/²³⁸U), in groundwater may also be used as a tracer for U mobility in the subsurface.³⁴ The ²³⁴U is the daughter of the short-lived decay product ²³⁴Th ($t_{1/2} = 24.1$ d) produced by α decay of ²³⁸U. In undisturbed U deposits older than ~1 million years, (²³⁴U/²³⁸U) should approach secular equilibrium (i.e., (²³⁴U/²³⁸U) = 1). (²³⁴U/²³⁸U) in sediments and groundwater

often deviates from secular equilibrium due to the complex interplay between α -recoil and dissolution of U minerals.³⁵ The ejection of an α -particle causes the daughter product ²³⁴Th to recoil a distance of ~30 nm in the lattice of silicate minerals.^{36,37} When the grain size is sufficiently small, this recoil may cause the ejection of ²³⁴Th and the daughter product ²³⁴U into the surrounding medium. In larger particles, the α -recoil tends to concentrate ²³⁴U at sites damaged by the decay process causing ²³⁴U to be preferentially leached during oxidative dissolution. Thus, the U mineral undergoing α -decay acquires a (²³⁴U/²³⁸U) less than unity, whereas the (²³⁴U/²³⁸U) of the surrounding groundwater is typically greater than 1.^{37,38} However, in open systems where the dissolved U is continuously removed, (²³⁴U/²³⁸U) in the groundwater may evolve to be lower than the secular equilibrium value.³⁹ A characterization of the (²³⁴U/²³⁸U) signature of the ore and the postmining groundwater is required for successful use of (²³⁴U/²³⁸U) activity ratios as tracer for U mobility at ISR sites.

Here, we report high precision measurements of $\delta^{238}\text{U}$, (²³⁴U/²³⁸U), and $\delta^{34}\text{S}$, and the elemental composition groundwater samples collected at an alkaline ISR mine (see the Supporting Information) from upgradient, within and downgradient of a roll-front type U deposit at Rosita, TX, USA. We also report U and S isotope measurements of U ore collected from an adjacent unmined part of the roll-front. Our objectives are to (i) detect naturally occurring reducing environments conducive to U(VI) reduction through isotopic and geochemical measurements and (ii) characterize the (²³⁴U/²³⁸U) of the U ore and the groundwater in order to use U activity ratios as a tracer for the migration of postmining groundwater from the ore zone.

MATERIALS AND METHODS

The study site is located at Rosita (Duval County), TX, USA, in the Texas coastal plain region. The ore deposit at the study site is divided into four mining units or production area authorizations (PAAs): PAA1, PAA2, PAA3, and yet-to-be mined PAA4 (Figure 1). The mining was carried out using the site groundwater fortified with NaHCO₃ and/or CO₂ (g) and oxidants (O₂, H₂O₂). We collected groundwater samples from 32 wells located upgradient, within, and downgradient of the roll-front ore in May 2013 (Figure 1). We obtained a sediment core from the ore zone (borehole OZCH3, adjacent to BL 39) within the unmined PAA4 area (Figure 1). Details of the site background, lithology (Figure S1), mining history, methods for sample collection, and major ion and trace element analysis are provided in the Supporting Information.

Isotopic Analyses. The ²³⁸U/²³⁵U measurements in groundwater and digested ore samples were performed at the Stanford ICP-MS/TIMS Facility, Stanford University, using a Nu Plasma multicollector-inductively coupled plasma mass spectrometry (MC-ICPMS) instrument following the methods described in refs 17 and 22–24. All samples were purified using UTEVA resin (Eichrom Technologies, LLC) prior to isotopic measurements. The measured ²³⁸U/²³⁵U ratios are expressed as $\delta^{238}\text{U}$ relative to the U isotope standard CRM 145, defined by

$$\delta^{238}\text{U} = \left[\frac{(^{238}\text{U}/^{235}\text{U})_{\text{sample}}}{(^{238}\text{U}/^{235}\text{U})_{\text{CRM145-A}}} - 1 \right] \times 1000\text{‰} \quad (1)$$

Analytical uncertainty of the isotope measurements was $\pm 0.09\text{‰}$, determined as 2 times the root-mean-square difference for 10 pairs of duplicate sample preparations.

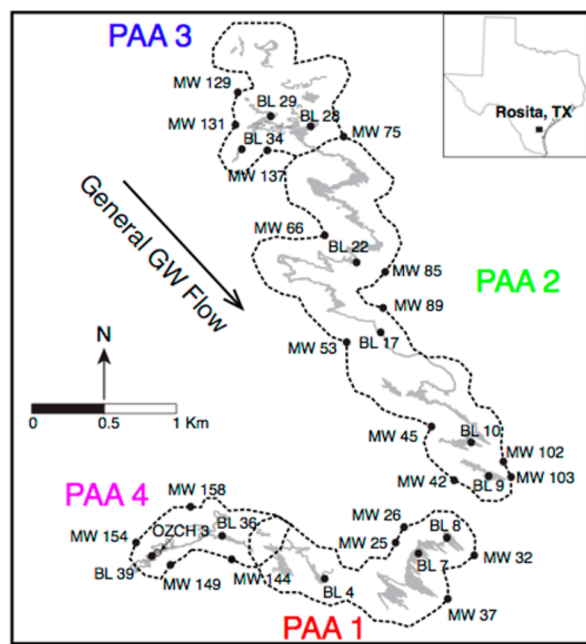


Figure 1. Map of the Rosita ISR site showing the sampling locations in the mining units (PAAs). The gray shaded area defines the U roll-front deposit. The dotted lines define the inferred PAA boundaries and the perimeter ring of the monitoring wells. Black dots show the sampling locations for the base line (BL) wells within the ore zone and upgradient and downgradient monitoring wells (MW). Arrow indicates the present groundwater flow direction. Open circle (OZCH3) shows the location of the U ore sample.

The ($^{234}\text{U}/^{238}\text{U}$) values were measured at the Center for Isotope Geochemistry, Lawrence Berkeley National Laboratory using an IsoProbe MC-ICPMS instrument (GV Instruments) following the method described in ref 40. For isotopic analyses, U was extracted from the samples using TRU Spec resin (Eichrom Technologies, LLC). The analytical precision (2σ) of the ($^{234}\text{U}/^{238}\text{U}$) was $<0.2\%$.

Sulfur isotope ratios in groundwater and ore samples were measured at the Laboratory for Environmental and Sedimentary Isotope Geochemistry, University of California, Berkeley on a Eurovector model 3028 elemental analyzer interfaced with a GV Isoprime isotope ratio mass spectrometer. Details on the sample preparation and measurement technique can be found in ref 41. The analytical uncertainty (2σ) for the isotope measurements was 0.15% , determined from the long-term measurements of S isotope standard NBS 127 and in house standards. We report the measured $^{34}\text{S}/^{32}\text{S}$ isotope ratios as $\delta^{34}\text{S}$, relative to that of the standard reference material Canyon Diablo Troilite, defined as

$$\delta^{34}\text{S} = \left[\frac{(^{34}\text{S}/^{32}\text{S})_{\text{sample}}}{(^{34}\text{S}/^{32}\text{S})_{\text{CDT}}} - 1 \right] \times 1000\text{‰} \quad (2)$$

We measured $\delta^{15}\text{N}$ and $\delta^{18}\text{O}$ (defined similarly as in the above equations) of NO_3^- in groundwater samples with >0.1 mg/L NO_3^- to detect any possible microbial denitrification. The $\delta^{15}\text{N}$ and $\delta^{18}\text{O}$ of NO_3^- were measured using a modified version of the microbial denitrification technique described in refs 42 and 43. Briefly, N_2O gas evolved following reduction of nitrate by *Pseudomonas aureofaciens* (ATCC 13985) was measured in continuous flow mode using a GV Instruments Isoprime isotope ratio mass spectrometer (GV Instruments, Manchester,

UK) coupled to a TraceGas peripheral instrument. Calibration was performed based on standards IAEA-NO-3, USGS32, and USGS34. Precision was typically $\pm 0.25\text{‰}$ for $\delta^{15}\text{N}$ and $\pm 0.90\text{‰}$ for $\delta^{18}\text{O}$.

The details of ore digestion procedure, major ion and trace element measurement methods, and Sr isotope measurements in Rosita groundwater are provided in the Supporting Information.

RESULTS AND DISCUSSION

Geochemistry and Isotope Geochemistry of Rosita Groundwater. The major ion and trace element chemistry of the groundwater samples are shown in Table S1 (es5b00701_si_002.xlsx) of the Supporting Information. The pH of Rosita groundwater samples measured during sample collection varies from 6.56 to 7.36. The dissolved organic carbon in the groundwater ranges from 0.66 to 6.28 mg/L, with a median value of 1.2 mg/L. In general, the groundwater samples are characterized by high concentrations of Na^+ (156–472 mg/L), Ca^{2+} (72–391 mg/L), Cl^- (341–1254 mg/L), HCO_3^- (190–379 mg/L), SO_4^{2-} (66–653 mg/L, median concentration 243 mg/L), and total dissolved solids (1045–3188 mg/L). U(VI) concentrations in the groundwater samples range from 0.001 to 12.9 mg/L, with the highest concentrations observed in the samples collected from the previously mined ore zone, particularly in samples BL 28, BL 29, and BL 34 from the most recently mined, and as of yet unrestored, PAA3. The redox potential (Eh) measured in groundwater samples varies from +94.2 to -105.5 mV. Some groundwater samples also contain a minor amount of dissolved Fe (up to 3.0 mg/L), Mn (up to 0.56 mg/L), and NO_3^- (up to 29.8 mg/L) (see Table S1 and Figure S2 of the Supporting Information). In addition, the samples from both previously mined and unmined ore zone BL wells contain dissolved Mo (0.003–3.41 mg/L; median concentration 0.39 mg/L).

The isotopic compositions of the groundwater samples are shown in Table S2 (es5b00701_si_003.xlsx) of the Supporting Information. A wide range of $\delta^{238}\text{U}$ values from $+0.61\text{‰}$ to -2.49‰ is observed in Rosita groundwater (Figure 2). Most of the ore zone groundwater samples are characterized by high $\delta^{238}\text{U}$ values ($\sim 0.0\text{‰} < \delta^{238}\text{U} < 0.61\text{‰}$), whereas the $\delta^{238}\text{U}$ of the groundwater from recently mined PAA3 and most of the upgradient wells are close to 0.0‰ . In contrast, most of the downgradient water samples are highly depleted in ^{238}U , exhibiting negative $\delta^{238}\text{U}$ values in the range -0.15‰ to -2.49‰ . In a subset of samples, a systematic decrease in $\delta^{238}\text{U}$ values is observed with decreasing U(VI) concentration that conforms to a Rayleigh distillation model with an ϵ of $0.48\text{‰} \pm 0.08\text{‰}$ (see Figure S3 of the Supporting Information).

The ($^{234}\text{U}/^{238}\text{U}$) in the groundwater samples from previously mined and unmined PAAs varies from 0.72 to 2.23 (see Table S2 of the Supporting Information and Figure 3). All ore zone wells, except BL 8, in the mined part of the roll-front exhibit a narrow range of ($^{234}\text{U}/^{238}\text{U}$), with an average value of ~ 0.75 . Except for five samples (MW 53, MW 75, MW 102, MW 129, and MW 137), ($^{234}\text{U}/^{238}\text{U}$) in both upgradient and downgradient wells are less than unity (Figure 3). In all transects (except the one containing BL 8), the ($^{234}\text{U}/^{238}\text{U}$) is lowest in the ore zone and higher, approaching secular equilibrium, in both the upgradient and downgradient wells.

We observed a wide range of $\delta^{34}\text{S}$ ($+11.8\text{‰}$ to -19.9‰) in aqueous sulfate from groundwater samples (see Table S2 of the Supporting Information). Most of the ore zone wells from

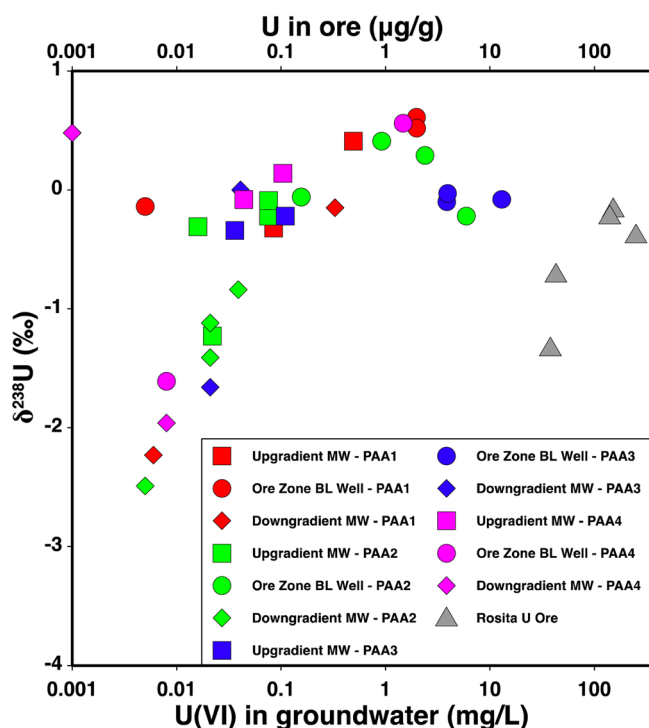


Figure 2. Measured $\delta^{238}\text{U}$ in Rosita groundwater and ore samples vs U concentration. Red, green, blue, and pink symbols represent the groundwater samples from PAA1, PAA2, PAA3, and unmined PAA4, respectively. Gray triangles represent the U ore samples from PAA4. The error bars (2 s.e.) for $\delta^{238}\text{U}$ do not exceed the size of the symbols.

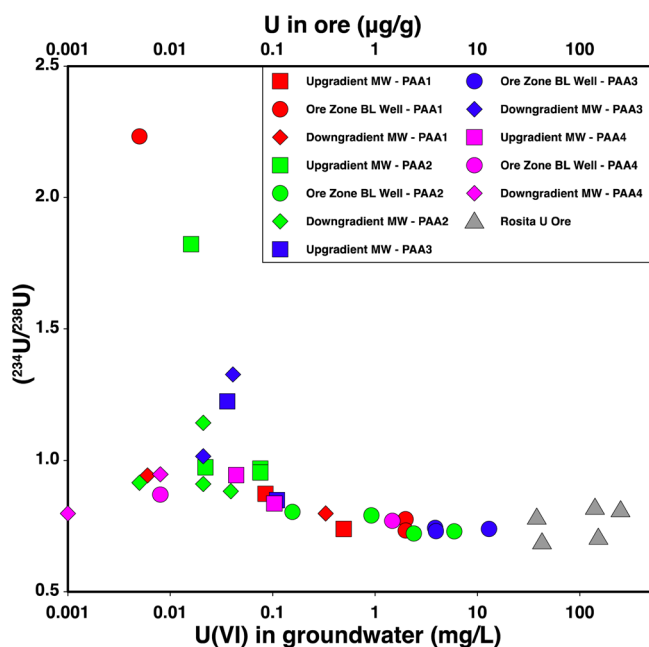


Figure 3. $(^{234}\text{U}/^{238}\text{U})$ vs U concentration in Rosita groundwater and ore samples. Red, green, blue, and pink symbols represent the groundwater samples from PAA1, PAA2, PAA3, and unmined PAA4, respectively. Gray triangles represent the U ore samples from PAA4. The error bars (2σ) for $(^{234}\text{U}/^{238}\text{U})$ are smaller than the size of the symbols.

previously mined PAA1, PAA2, and PAA3, except BL 8, BL 17, and BL 10, are depleted in aqueous ^{34}S (i.e., $\delta^{34}\text{S} \ll 0.0\text{‰}$). Among these, the most depleted $\delta^{34}\text{S}$ values are observed in

samples from the most recently mined PAA3. Most upgradient and downgradient samples, in contrast, have $\delta^{34}\text{S}$ near 0.0‰ or more enriched values up to $\sim 12\text{‰}$ (except in MW 25 and MW 85). In the unmined PAA4, $\delta^{34}\text{S}$ values in all samples (upgradient, ore zone, and downgradient) are enriched ($>0.0\text{‰}$) and fall within a narrow range (3.17‰ to 6.56‰). The $^{87}\text{Sr}/^{86}\text{Sr}$ ratios measured in groundwater from the mined PAA1, PAA2, and PAA3, vary from 0.7076 to 0.7081 (see Figure S4 of the Supporting Information).

Isotope Geochemistry of Rosita U Ore. Isotopic analyses of Rosita U ore, collected from the borehole OZCH3, in the unmined PAA4 area (Figure 1), are provided in Table S2 of the Supporting Information. We analyzed samples from four discrete depths across the uranium rich zones as identified by prompt fission neutron measurements in the borehole. The U ore is isotopically heterogeneous with $\delta^{238}\text{U}$ values from -0.16‰ to -1.33‰ and concentrations ranging from 38 to 250 mg kg^{-1} . Despite the variability in $\delta^{238}\text{U}$, the weighted average $\delta^{238}\text{U}$ for the U ore is -0.31‰ . The $(^{234}\text{U}/^{238}\text{U})$ values are also extremely low (0.69 to 0.82; average 0.76) in these samples, and tend to increase with depth. We observed highly depleted $\delta^{34}\text{S}$ values (-28.5‰ to -38.8‰) in the ore. There is no clear relationship between depth and $\delta^{238}\text{U}$ or $\delta^{34}\text{S}$.

Fractionation of ^{238}U and U(VI) Removal in Reducing Zones. The systematic decrease in $\delta^{238}\text{U}$ with U(VI) concentration in Rosita groundwater suggests naturally occurring U(VI) reduction as the major U removal process, particularly in areas downgradient of the roll-front. Correlations between the $\delta^{238}\text{U}$ and concentration exclude dilution as the explanation for low U concentrations in the downgradient region (Figure 2). Dissolution of the ore could affect the $\delta^{238}\text{U}$ in Rosita groundwater but appears negligible for the following reason: the $\delta^{238}\text{U}$ values (as low as -2.49‰) in groundwater from several downgradient monitoring wells are much more depleted than those observed in the U ore (Figure 2). Therefore, dissolution of U ore cannot solely account for the observed distribution of U isotopic fractionation in the downgradient water samples. Adsorption, as the major nonreductive U(VI) removal process, is unlikely due to the abundance of dissolved calcium ($72\text{--}391 \text{ mg/L}$ or $1.8\text{--}9.8 \text{ mM}$) and HCO_3^- ($190\text{--}379 \text{ mg/L}$ or $3.1\text{--}6.2 \text{ mM}$) in the site groundwater. Under these conditions, calcium–uranyl–carbonate complexes ($\text{Ca}_2\text{UO}_2(\text{CO}_3)_3^0_{\text{aq}}$ and $\text{CaUO}_2(\text{CO}_3)_3^{2-}$) become dominant U species⁴⁴ at near-neutral to slightly alkaline pH values and substantially decrease the adsorption of U(VI) onto mineral grains.^{45–51} A minor amount of adsorption of U(VI) may still occur, but adsorption–desorption does not cause U isotope fractionation.²⁴ In addition, U(VI) reduction is uninhibited and thermodynamically favorable at high HCO_3^- and Ca^{2+} .^{52,53}

The only mechanism known to induce large U isotope fractionation is the reduction of U(VI) to U(IV). The overall variation of $\delta^{238}\text{U}$ in Rosita groundwater is 3.1‰ , which is a factor of 3 higher than that observed during U(VI) bioremediation experiments at the U.S. Department of Energy's Integrated Field Research Challenge (IFRC) site at Rifle, Colorado, USA²² and similar to the overall change in $\delta^{238}\text{U}$ reported for groundwater samples from the Pepegona sandstone-hosted U deposit, Australia,²¹ and for microbial reduction of U(VI) in batch incubation experiments.²³ Furthermore, for all transects, except the one containing BL8, in the previously mined PAAs, the $\delta^{238}\text{U}$ and U(VI) concentrations decrease along the putative redox gradient

from the ore zone to downgradient monitoring wells, suggesting greater extents of U(VI) reduction and concomitant isotopic fractionation in (presumably) more reducing environments downgradient of the ore zone.

Additional geochemical data from the previously mined PAAs are consistent with the reducing environments identified based on the U isotope ratios. Along a groundwater flow path, a sequential zonation of terminal electron acceptors (e.g., O_2 , NO_3^- , Mn(IV)) based on energetic favorability of microbially mediated redox processes is often observed in aquifers.^{54,55} The sequence of reduction depends on the prevailing redox potential (Eh) and is usually as follows $O_2 > NO_3^- > Mn(IV) > Fe(III) > SO_4^{2-} > CO_2$. Under certain conditions, the concentrations of the soluble products of these reduction reactions (i.e., Mn^{2+} or Fe^{2+}) may be used to identify the terminal electron accepting process (i.e., Mn(IV) or Fe(III) reduction).⁵⁴

We observe a decrease in NO_3^- concentrations along the hydraulic gradient excluding the wells located downgradient of mapped gaps in the ore deposit that suggest heterogeneities in flow and mineral distribution (MW 32, MW 102, MW 103, MW 137; Figure 1). Despite the absence of a clear trend of decreasing NO_3^- concentrations with increasing $\delta^{15}N$ -nitrate, the $\delta^{18}O$ -nitrate vs $\delta^{15}N$ -nitrate plot shows a linear relation ($r^2 = 0.77$, $n = 11$) with a slope ($\Delta\delta^{18}O/\Delta\delta^{15}N$) of 0.73 ± 0.13 similar to that characteristic of microbial denitrification,^{56–61} particularly in the upgradient wells in the previously mined parts of the site (see Figure S5 of the Supporting Information). The above-mentioned gaps in the ore deposit at the southernmost part of PAA2 and in PAA3 (Figure 1) enable the nitrate-rich groundwater to arrive at the downgradient wells MW 32, MW 102, MW 103, and MW 137. In this process, the upgradient water also dilutes the U(VI) concentrations in the downgradient wells on its flow path. Dissolved Mn (>0.05 mg/L) and Fe (>0.1 mg/L) concentrations in Rosita groundwater additionally suggest localized zones of Mn(IV) and Fe(III) reduction in PAA1, PAA2, and PAA3 (see Figure S2 of the Supporting Information).

The general trend in Eh coincides with the distribution of NO_3^- , Fe, and Mn concentrations in Rosita groundwater. The Eh values (+94.2 to -105.5 mV) in Rosita groundwater suggest a wide range of likely redox reactions such as denitrification, Mn(IV), Fe(III), and U(VI) reduction (occurring below 0.0 mV at pH 7),⁴⁴ but are higher than that required for sulfate reduction (≤ -200 mV).^{44,54,62,63} We observe an apparent trend of decreasing Eh values downgradient of the ore zone in the previously mined PAAs; high Eh values (-30 to $+90$ mV) are mostly associated with the upgradient and ore zone wells where various degrees of oxidation are expected (see Figure S2 of the Supporting Information). Most of the downgradient wells (except MW 32, MW 102, MW 103, MW 137) in all previously mined PAAs show low to very low Eh values, suggesting reducing environments. At near-neutral pH, the zones of Fe(III) reduction along with very low Eh values (~ -100 mV) suggest the presence of reducing environments favorable for U(VI) reduction.^{44,63}

The concurrent decrease of $\delta^{238}U$ and U(VI) in groundwater along the hydraulic gradient can be modeled using a Rayleigh distillation relationship. In our calculation of ϵ , we excluded the wells affected by dilution, either by the upgradient water as evident from the nitrate plume (e.g., at the boundary of PAA1 and PAA2) or by the most recent mining activity in PAA3. We also excluded MW 149 (PAA4), in which ^{238}U enrichment

($\delta^{238}U = 0.48\%$) similar to the corresponding ore zone well BL 39 suggests a lack of U(VI) reduction. The U(VI) data from the wells affected by nonreductive U removal, dilution or dissolution would lead to an error in estimating the relationship between the remaining unreduced U(VI) and the accompanying $\delta^{238}U$ and thus in the estimation of the ϵ in the Rayleigh distillation model. The fit of the data from the 14 remaining wells, including the PAA4 wells, yields an ϵ value of 0.48% (see Figure S3 of the Supporting Information). The magnitude of U isotope fractionation (ϵ) in Rosita groundwater is very similar to that determined for microbial U(VI) at the Rifle biostimulation site ($\epsilon \approx 0.46\%$),²² and about a factor of 2 less than that observed during microbial U(VI) reduction in batch incubation experiments ($\epsilon \approx 1.0\%$).²³ Because Rayleigh distillation models presuppose a closed system with no back reaction, applicability of these models to determine the magnitude of U isotope fractionation during U(VI) reduction in aquifers is somewhat uncertain and hydrodynamic dispersion and diffusion can lead to underestimation of the fractionation factors.⁶⁴ In addition, field scale chemical heterogeneity at the Rifle biostimulation site and at Rosita might have resulted in a diffusive limitation between the isolated zones of U(VI) reduction leading to less apparent fractionation compared to that observed during U(VI) reduction in well-mixed batch incubation experiments.^{65,66} Alternatively, different U(VI) reduction mechanism(s) at Rosita might have generated the difference in ϵ with previously published studies.

Several groundwater samples from the ore zone and upgradient wells, both from the previously mined and unmined parts of the site, show ^{238}U enrichment ($0.0\% < \delta^{238}U < 0.61\%$) relative to the U ore collected from OZCH-3 in PAA4. For example, $\delta^{238}U$ in groundwater from BL 39 from unmined PAA4 is much higher than that of the U ore ($\delta^{238}U$ at highest U concentration = -0.22%) obtained from the adjacent borehole OZCH-3. The U isotope fractionation in this case is opposite to that observed during U(VI) reduction or equilibrium isotopic fractionation between U(IV) and U(VI) (i.e., ^{235}U enrichment in the dissolved U(VI)).

The mechanism(s) responsible for enrichment of ^{238}U in the groundwater is unclear. It is unlikely that U mineral dissolution gives rise to these anomalous $\delta^{238}U$ in the groundwater, as several recent studies demonstrated lack of isotope fractionation during progressive leaching of U minerals.^{18–20} However, it is not known whether oxidation of U(IV) to U(VI) during incongruent dissolution of U minerals induces any isotopic fractionation. Brennecka et al. (2011) reported a small isotopic fractionation ($\sim 0.2\%$) during adsorption of U(VI) on Mn-oxyhydroxides in experiments at pH ~ 5 using a diluted U solution equilibrated with atmospheric CO_2 , where preferential adsorption of ^{235}U led to an enrichment of ^{238}U in the remaining dissolved U(VI).⁶⁷ These experimental conditions greatly differ from the near neutral to slightly alkaline Rosita groundwater with abundant dissolved Ca (>72 mg/L or 1.8 mM) and bicarbonate (>190 mg/L or 3.1 mM), which should render the adsorption of U(VI) less effective and minor. Because U(VI) reduction produces ^{238}U enriched U(IV) minerals, remobilization of isotopically heavy U ore ($\delta^{238}U > 0.0\%$) resulting from prior U redox cycling may produce ^{238}U enriched groundwater. The $\delta^{238}U$ of the U ore from a single core (OZCH-3 in PAA4) does not show the enriched values expected for U that has been enriched by prior redox cycling; however, we cannot assess the spatial variability in the extent of ^{238}U enrichment based on the limited measurements. There-

fore, further investigation is required to determine ^{238}U enrichment mechanisms.

U Attenuation and Reducing Environments in Unmined PAA4. The geochemical and isotope data from groundwater and sediment samples from the unmined PAA4 area provide some key insights into the naturally occurring processes that can be used as a proxy for the premining U cycling at the study site. In the unmined area, dissolved oxidants (e.g., oxygen, nitrate) in recharge groundwater interact with the reducing environments in and downgradient of the ore deposit. This process should lead to consumption of the oxidants as the packet of water moves through progressively more reduced zones. Our results showed this general trend despite spatial heterogeneity at the study site. For example, NO_3^- concentrations decreased from 12 to 15 mg/L in the upgradient water (MW 158, MW 154) to below detection (<0.1 mg/L) in the ore zone or in the downgradient samples in PAA4 (Table S1 of the Supporting Information). In addition, elevated concentrations of dissolved Fe and Mn (see Table S1 of the Supporting Information) in the ore zone and downgradient wells compared to those in the upgradient wells suggest subsurface environments conducive to Fe(III) and Mn(IV) reduction. The distribution of U(VI) in groundwater samples is heterogeneous; U dissolution is suggested by elevated U(VI) in the upgradient wells in both transects and in BL 39 (U(VI) = 1.47 mg/L) whereas the groundwater samples from the downgradient wells are characterized by very low U(VI) (<0.008 mg/L). This decrease in U(VI) in the downgradient water presumably results from U(VI) reduction somewhere between the ore deposit and the downgradient location.

Although U(VI) concentration data provide no clear information on the distribution of reducing environments, U isotope ratios in groundwater may indicate U(VI) reduction in the PAA4 area. The U(VI) in samples from the eastern transect (MW 158, BL 36, MW 144) becomes increasingly enriched in ^{235}U (lowered $\delta^{238}\text{U}$ from -0.08% to -1.91%). Highly depleted $\delta^{238}\text{U}$ (-1.91%) observed in the sample from MW 144 cannot be produced by dissolution of the isotopically light fraction ($\delta^{238}\text{U} = -1.33\%$) of the ore. This suggests progressive U(VI) reduction along this transect. In contrast, $\delta^{238}\text{U}$ of all groundwater samples from the western transect (MW 154, BL 39, MW 149) are elevated with the highest $\delta^{238}\text{U}$ (0.56%) and the highest U(VI) concentration (1.47 mg/mL) in PAA4 observed in BL 39, suggesting dissolution of the U ore and a lack of U(VI) reducing environments along this transect. This heterogeneous distribution of $\delta^{238}\text{U}$ in groundwater PAA4 suggests field scale heterogeneity in the distribution of naturally occurring reducing environments.

($^{234}\text{U}/^{238}\text{U}$) at Rosita. Extremely low ($^{234}\text{U}/^{238}\text{U}$) ranging from 0.69 to 0.82 in the Rosita U ore can be generated by (1) direct ejection of ^{234}U from the U mineral grains into the surrounding medium (i.e., groundwater) due to α -recoil, leading to a steady state depletion of ^{234}U in the U mineral grains and (2) preferential dissolution of ^{234}U from the recoil-damaged lattice sites of U-bearing minerals. The fraction of ^{234}U ejected (f_a) directly from the U mineral into the surrounding medium is a function of size and geometry of mineral grains, and increases with decreasing grain size.^{38,68,69} If only direct recoil of ^{234}U is responsible for the observed ^{234}U depletion ($(^{234}\text{U}/^{238}\text{U}) \approx 0.75$), a corresponding ^{234}U loss factor or f_a of 0.25 is required. This value of f_a is expected only in sediments with a very fine grain size ($0.2\text{--}2\ \mu\text{m}$).⁶⁸ The

mean grain diameter of the 50% of the U minerals (D_{50}) in the Rosita ore is $12\ \mu\text{m}$ (see Table S3 of the Supporting Information). However, it is not uncommon that the amount of recoil loss is larger than expected based on the geometric grain radius, probably due to grain surface roughness.⁶⁹ Furthermore, in U minerals, the extensive radioactive decay of U and intermediate daughter isotopes would likely result in much more lattice damage than observed in silicate minerals. Pervasive lattice damage may enhance preferential dissolution of ^{234}U in U minerals. Therefore, both direct recoil and dissolution of ^{234}U from the damaged lattice sites likely gave rise to observed ^{234}U depletion in the Rosita ore.

In many aquifers, the ($^{234}\text{U}/^{238}\text{U}$) of the groundwater reflects a balance between the supply of ^{234}U from α -recoil, preferential leaching, and the dissolution of the solids, which may contain ^{234}U depleted surfaces.³⁴ The ore zone groundwater samples, except BL 8, exhibit the extreme ^{234}U depletion and ($^{234}\text{U}/^{238}\text{U}$) similar (average ($^{234}\text{U}/^{238}\text{U}$) = 0.76 ± 0.03 , $n = 9$) to that of the U ore. The average ($^{234}\text{U}/^{238}\text{U}$) values of the ore zone groundwater are within the uncertainty of that for the ore samples suggesting that dissolution within ore deposit is much more important than direct recoil of ^{234}U . Very high U content in U ore relative to that in groundwater results in a rapid shift in the isotopic composition toward that of the high-U solid in the ore zone. In contrast, Rosita groundwater samples with lower U concentrations have higher ($^{234}\text{U}/^{238}\text{U}$), consistent with aquifers where α -recoil dominates over dissolution of U from the bulk solids with lower U concentrations.^{34,70,71} Thus, the ($^{234}\text{U}/^{238}\text{U}$) composition of the ore zone groundwater adjusts to the value of the ore deposit, providing a means to trace ore zone water.

The spatial variation of ($^{234}\text{U}/^{238}\text{U}$) in groundwater along the hydraulic gradient may be understood using the framework described above. Compared to the ore zone groundwater, samples from the upgradient wells are more enriched in ^{234}U , but with ($^{234}\text{U}/^{238}\text{U}$) closer to the secular equilibrium value of 1, except in MW 129 and MW 53. The sediments upgradient of the ore zone have trace U concentrations primarily hosted in silicate minerals and possibly in residual U minerals, deposited prior to the downgradient movement of the roll-front to its present location. In these older sediments with a low U content, α -recoil within the aquifer along with low rates of mineral dissolution might give rise to the slight ^{234}U enrichment in groundwater in the upgradient wells.^{70,71} Downgradient groundwater samples also show ^{234}U enrichment compared to the ore zone wells but are generally below secular equilibrium. This ^{234}U enrichment may be attributed primarily to the ^{234}U contribution from the downgradient sediments during transport. Typically, under premining conditions, as the water exits the ore deposit, the U(VI) is reduced almost quantitatively toward the downgradient reduced edge of the roll-front. Sediments located further downgradient should have a U budget that is primarily in silicate minerals similar to the upgradient sediments. Thus, due to efficient U removal over a relatively short distance from the ore zone, the ($^{234}\text{U}/^{238}\text{U}$) in the advecting water largely differs from that of the ore zone and evolves to a near secular equilibrium value during transport to the downgradient wells. At present, any influence of the ore zone groundwater with extremely low ($^{234}\text{U}/^{238}\text{U}$) is unlikely in the downgradient samples, as $^{87}\text{Sr}/^{86}\text{Sr}$ ratios (see Figure S4 of the Supporting Information) suggest no apparent mixing between waters from the ore zone and downgradient wells.

($^{234}\text{U}/^{238}\text{U}$) as Tracer for U Migration. ($^{234}\text{U}/^{238}\text{U}$) in groundwater may be used to track U mobility along groundwater flow. Given the present groundwater velocity of 3 to 6 m yr^{-1} at the site, it is unlikely that the postmining restoration fluid has arrived at the downgradient monitoring wells, located approximately 200 m from the ore zone, since the cessation of the ISR mining between 1997 and 1999. In absence of efficient reduction of postrestoration high U(VI), the arrival of the ore zone water at the downgradient wells can be traced using the characteristic ($^{234}\text{U}/^{238}\text{U}$) (≈ 0.76) of the ore zone water. Therefore, if high U(VI) ore zone water escapes, it will have a unique ($^{234}\text{U}/^{238}\text{U}$) signature that will persist according to the U(VI) concentration and the efficiency of (1) mixing with other water and (2) α -recoil and leaching processes downstream.

S Isotopes as Tracers for Reduction and Groundwater Movement. The $\delta^{34}\text{S}$ values of sulfate in groundwater can help us identify the processes influencing U mobility. Extremely depleted $\delta^{34}\text{S}$ of the Rosita U ore (-28.5% to -38.8%) is similar to that reported for South Texas U ores (summarized in ref 8). These very low $\delta^{34}\text{S}$ values are generally attributed to redistribution of preore FeS_2 produced by microbial sulfate reduction and mixing of groundwater with sulfur-enriched brine.⁸ Although the $\delta^{34}\text{S}$ values in sulfate in Rosita groundwater vary over a wide range ($+11.8\%$ to -19.9%) (see Figure S6 of the Supporting Information), there is no systematic relationship between $\delta^{34}\text{S}$ and SO_4^{2-} concentrations in Rosita groundwater. When plotted against the groundwater U(VI) concentrations, a proxy for degree of dissolution and reduction, $\delta^{34}\text{S}$ in most of the ore zone BL wells plot in the same region (see Figure S6 of the Supporting Information). The characteristic depleted $\delta^{34}\text{S}$ values in ore zone groundwater likely result from the oxidative dissolution of sulfide minerals during which $\delta^{34}\text{S}$ in sulfate approaches the isotopic signature of the source sulfide. This dissolution signature is most prominent in samples from recently mined PAA3 ($\delta^{34}\text{S} = -14.8\%$ to -19.9%).

The elevated $\delta^{34}\text{S}$ in aqueous sulfate is not likely to arise from microbial sulfate reduction and is consistent with mixing with ^{34}S enriched background water. The $\delta^{34}\text{S}$ values in groundwater from the PAA4, ranging from 3.2% to 6.6%, are significantly elevated above that in PAA3 wells. We did not observe any large decrease in aqueous sulfate concentration or concomitant enrichment in $\delta^{34}\text{S}$ from ore zone to downgradient wells in PAA4. This suggests that $\delta^{34}\text{S}$ of aqueous sulfate in PAA4 represent the background S isotope signature of the site groundwater. In the mined part of the site, the samples with considerably high $\delta^{34}\text{S}$ enrichment up to 12% (e.g., BL 10, MW 45, MW 53, MW 102, MW 103, MW 137) also contain more than 12 mg/L NO_3^- , which precludes microbial sulfate reduction in these wells. The $\delta^{34}\text{S}$ in several downgradient samples, particularly in MW 37, MW 75, MW 89, and MW 137, approach 0.0% or occasionally higher values. In these wells, the redox potentials do not decrease below -105.5 mV and do not reach sulfate reducing conditions. Therefore, the elevated $\delta^{34}\text{S}$ in the mined part of the site is not indicative of sulfate reducing environments. However, we cannot completely rule out a minor amount of localized SO_4^{2-} reduction.

The characteristic depleted $\delta^{34}\text{S}$ of the ore zone wells may also be used as a tracer for the downgradient migration of the ore zone groundwater. However, any SO_4^{2-} reduction along the groundwater flow path would lead to enrichment of ^{34}S in the

residual sulfate which would be difficult to distinguish from mixing with the downgradient groundwater enriched in ^{34}S . At present, we do not have any isotopic or geochemical evidence of major sulfate reducing areas in either unmined or mined parts of the site, consistent with the measured Eh values. In the absence of substantial SO_4^{2-} reduction along the hydraulic gradient, characteristic S isotope ratios could be used to trace the mobility of the ore zone groundwater.

Implications for U Remediation at Rosita ISR Site. In the majority of the downgradient wells, lower $\delta^{238}\text{U}$ relative to the U ore and ore zone groundwater, accompanied by a decrease in U(VI) concentration, strongly suggest naturally occurring U(VI) reduction downgradient of the ore zone. Our results also suggest progressively stronger reducing environments ranging from nitrate to iron reducing conditions along the hydraulic gradient. The characteristic ($^{234}\text{U}/^{238}\text{U}$) signature may serve as a monitoring tool to trace fugitive ore zone water at Rosita in case of incomplete U(VI) reduction in the reducing environments located downgradient of the ore zone. Additionally, $\delta^{34}\text{S}$ signature may also be used as a tracer for the mobility of the ore zone groundwater. Overall, the implications of our findings should extend to all ISR sites similar to Rosita. Although the isotopic and geochemical data from Rosita groundwater are effective in detecting naturally occurring U(VI) reduction at the ISR site, these data do not reveal the mechanism or the extent of U(VI) reduction. Future investigation will determine the potential, kinetics, and associated isotopic fractionation for U(VI) reduction in the downgradient sediments.

■ ASSOCIATED CONTENT

● Supporting Information

Details of the site background, analytical procedures, groundwater major ion and trace element concentrations, and isotopic data ($\delta^{238}\text{U}$, ($^{234}\text{U}/^{238}\text{U}$), $\delta^{34}\text{S}$, $\delta^{15}\text{N}$, and $\delta^{18}\text{O}$, $^{87}\text{Sr}/^{86}\text{Sr}$). The Supporting Information is available free of charge on the ACS Publications website at DOI: 10.1021/acs.est.5b00701.

■ AUTHOR INFORMATION

Corresponding Author

*A. Basu. Department of Earth and Planetary Science, 483 McCone Hall, University of California, Berkeley, Berkeley, CA 94720, USA. Phone: +1 (510) 643 5062. Fax: +1 (510) 642 9520. E-mail address: anirbanbasu@berkeley.edu.

Notes

The authors declare no competing financial interest.

■ ACKNOWLEDGMENTS

This research was funded by the UC Laboratory Fees Research Program. We thank Uranium Resources, Inc. for providing site access and logistic support during this investigation. We thank Karrie Weaver (Stanford University), Doug Ware, Michael Rearick, Emily Kluk, and George Perkins at Los Alamos National Laboratory for analytical support.

■ REFERENCES

- (1) Abzalov, M. Z. Sandstone-hosted uranium deposits amenable for exploitation by in situ leaching technologies. *Trans. Inst. Min. Metall., Sect. B* **2012**, *121* (2), 55–64.
- (2) Mudd, G. Critical review of acid in situ leach uranium mining: 1. USA and Australia. *Environ. Geol.* **2001**, *41*, 390–403.
- (3) Mudd, G. M. The future of Yellowcake: A global assessment of uranium resources and mining. *Sci. Total Environ.* **2014**, *472*, 590–607.

- (4) Mudd, G. M.; Diesendorf, M. Sustainability of uranium mining and milling: toward quantifying resources and eco-efficiency. *Environ. Sci. Technol.* **2008**, *42*, 2624–2630.
- (5) Schneider, E.; Carlsen, B.; Tavrides, E.; van der Hoeven, C.; Phathanapirom, U. A top-down assessment of energy, water and land use in uranium mining, milling, and refining. *Energy Econ.* **2013**, *40*, 911–926.
- (6) *Uranium: Cradle to Grave*; Fayek, M., Burns, P. C., Sigmon, G., Eds.; Short Course Series; Mineralogical Association of Canada: Quebec, QC, 2013; Vol. 43, pp 121–146.
- (7) Hazen, R. M.; Ewing, R. C.; Sverjensky, D. A. Evolution of uranium and thorium minerals. *Am. Mineral.* **2009**, *94*, 1293–1311.
- (8) Dahlkamp, F. J. *Uranium Deposits of the World*; Springer: Berlin, Germany, 2009.
- (9) *Uranium 2011: Resources, Production and Demand*; A joint report by the OECD Nuclear Energy Agency and the International Atomic Energy Agency: Paris, France, 2012; <http://www.oecd-nea.org/ndd/pubs/2012/7059-uranium-2011.pdf>.
- (10) Ceyhan, M. *World Distribution of Uranium Deposits (UDEPO) with Uranium Deposit Classification*; IAEATECDOC-1629; Nuclear Fuel Cycle and Materials Section, International Atomic Energy Agency: Vienna, Austria, 2009; http://www-pub.iaea.org/MTCD/publications/PDF/te_1629_web.pdf.
- (11) Shawe, D. R.; Granger, H. C. Uranium ore rolls; an analysis. *Econ. Geol.* **1965**, *60*, 240–250.
- (12) Hobday, D. K.; Galloway, W. E. Groundwater processes and sedimentary uranium deposits. *Hydrogeol. J.* **1999**, *7*, 127–138.
- (13) Schauble, E. A. Role of nuclear volume in driving equilibrium stable isotope fractionation of mercury, thallium, and other very heavy elements. *Geochim. Cosmochim. Acta* **2007**, *71*, 2170–2189.
- (14) Bigeleisen, J. Nuclear size and shape effects in chemical reactions. Isotope chemistry of the heavy elements. *J. Am. Chem. Soc.* **1996**, *118*, 3676–3680.
- (15) Moynier, F.; Fujii, T.; Brennecke, G. A.; Nielsen, S. G. Nuclear field shift in natural environments. *C. R. Geosci.* **2013**, *345*, 150–159.
- (16) Abe, M.; Suzuki, T.; Fujii, Y.; Hada, M.; Hirao, K. An ab initio molecular orbital study of the nuclear volume effects in uranium isotope fractionations. *J. Chem. Phys.* **2008**, *129*, No. 164309.
- (17) Weyer, S.; Anbar, A. D.; Gerdes, A.; Gordon, G. W.; Algeo, T. J.; Boyle, E. A. Natural fractionation of $^{238}\text{U}/^{235}\text{U}$. *Geochim. Cosmochim. Acta* **2008**, *72*, 345–359.
- (18) Stirling, C. H.; Andersen, M. B.; Potter, E.-K.; Halliday, A. N. Low-temperature isotopic fractionation of uranium. *Earth. Planet. Sci. Lett.* **2007**, *264*, 208–225.
- (19) Brennecke, G. A.; Borg, L. E.; Hutcheon, I. D.; Sharp, M. A. Natural variations in uranium isotope ratios of uranium ore concentrates: Understanding the $^{238}\text{U}/^{235}\text{U}$ fractionation mechanism. *Earth. Planet. Sci. Lett.* **2010**, *291*, 228–233.
- (20) Bopp, C. J., IV; Lundstrom, C. C.; Johnson, T. M.; Glessner, J. J. Variations in $^{238}\text{U}/^{235}\text{U}$ in uranium ore deposits: Isotopic signatures of the U reduction process? *Geol.* **2009**, *37*, 611–614.
- (21) Murphy, M. J.; Stirling, C. H.; Kaltenbach, A.; Turner, S. P.; Schaefer, B. F. Fractionation of $^{238}\text{U}/^{235}\text{U}$ by reduction during low temperature uranium mineralisation processes. *Earth. Planet. Sci. Lett.* **2014**, *388*, 306–317.
- (22) Bopp, C. J., IV; Lundstrom, C. C.; Johnson, T. M.; Sanford, R. A.; Long, P. E.; Williams, K. H. Uranium $^{238}\text{U}/^{235}\text{U}$ isotope ratios as indicators of reduction: Results from an in situ biostimulation experiment at Rifle, Colorado, U.S.A. *Environ. Sci. Technol.* **2010**, *44*, 5927–5933.
- (23) Basu, A.; Sanford, R. A.; Johnson, T. M.; Lundstrom, C. C.; Löffler, F. E. Uranium isotopic fractionation factors during U(VI) reduction by bacterial isolates. *Geochim. Cosmochim. Acta* **2014**, *136*, 100–113.
- (24) Shiel, A. E.; Laubach, P. G.; Johnson, T. M.; Lundstrom, C. C.; Long, P. E.; Williams, K. H. No measurable changes in $^{238}\text{U}/^{235}\text{U}$ due to desorption–adsorption of U(VI) from groundwater at the Rifle, Colorado, Integrated Field Research Challenge Site. *Environ. Sci. Technol.* **2013**, *47*, 2535–2541.
- (25) Granger, H. C.; Warren, C. G. Unstable sulfur compounds and the origin of roll-type uranium deposits. *Econ. Geol.* **1969**, *64*, 160–171.
- (26) Rackley, R. I. Environment of Wyoming tertiary uranium deposits. *Mt. Geol.* **1972**, *9*, 143–157.
- (27) Harshman, E. N. Genetic implications of some elements associated with uranium deposits, Shirley Basin, Wyoming. *Geol. Surv. Res.* **1966**, C167–C173.
- (28) Reynolds, R. L.; Goldhaber, M. B. Iron disulfide minerals and the genesis of roll-type uranium deposits. *Econ. Geol.* **1983**, *78*, 105–120.
- (29) Fischer, R. P. Similarities, differences, and some genetic problems of the Wyoming and Colorado plateau types of uranium deposits in sandstone. *Econ. Geol.* **1970**, *65*, 778–784.
- (30) Jensen, M. L. Sulfur isotopes and the origin of sandstone-type uranium deposits [Colorado Plateau and Wyoming]. *Econ. Geol.* **1958**, *53*, 598–616.
- (31) Howard, J. H. Geochemistry of selenium: Formation of ferroselite and selenium behavior in the vicinity of oxidizing sulfide and uranium deposits. *Geochim. Cosmochim. Acta* **1977**, *41*, 1665–1678.
- (32) Canfield, D. E. Biogeochemistry of sulfur isotopes. In *Stable Isotope Geochemistry*; Valley, J. W., Cole, D. R., Eds.; Mineralogical Society of America: Washington, DC, 2001; pp 607–636.
- (33) Harrison, A. G.; Thode, H. G. The kinetic isotope effect in the chemical reduction of sulphate. *Trans. Faraday Soc.* **1957**, *53*, 1648–1651.
- (34) Porcelli, D.; Swarzenski, P. W. The behavior of U- and Th-series nuclides in groundwater. In *Uranium-Series Geochemistry*; Bourdon, B., Henderson, G. M., Lundstrom, C. C., Turner, S. P., Eds.; Mineralogical Society of America: Washington, DC, 2003; pp 317–361.
- (35) Maher, K.; Steefel, C. I.; DePaolo, D. J.; Viani, B. E. The mineral dissolution rate conundrum: Insights from reactive transport modeling of U isotopes and pore fluid chemistry in marine sediments. *Geochim. Cosmochim. Acta* **2006**, *70*, 337–363.
- (36) Maher, K.; DePaolo, D. J.; Christensen, J. N. U–Sr isotopic speedometer: Fluid flow and chemical weathering rates in aquifers. *Geochim. Cosmochim. Acta* **2006**, *70*, 4417–4435.
- (37) Kigoshi, K. Alpha-recoil thorium-234: Dissolution into water and the uranium-234/uranium-238 disequilibrium in nature. *Science* **1971**, *173*, 47–48.
- (38) DePaolo, D. J.; Maher, K.; Christensen, J. N.; McManus, J. Sediment transport time measured with U-series isotopes: Results from ODP North Atlantic drift site 984. *Earth. Planet. Sci. Lett.* **2006**, *248*, 394–410.
- (39) Andersen, M. B.; Erel, Y.; Bourdon, B. Experimental evidence for ^{234}U – ^{238}U fractionation during granite weathering with implications for $^{234}\text{U}/^{238}\text{U}$ in natural waters. *Geochim. Cosmochim. Acta* **2009**, *73*, 4124–4141.
- (40) Christensen, J. N.; Dresel, P. E.; Conrad, M. E.; Maher, K.; DePaolo, D. J. Identifying the sources of subsurface contamination at the Hanford site in Washington using high-precision uranium isotopic measurements. *Environ. Sci. Technol.* **2004**, *38*, 3330–3337.
- (41) Druhan, J. L.; Steefel, C. I.; Conrad, M. E.; DePaolo, D. J. A large column analog experiment of stable isotope variations during reactive transport: I. A comprehensive model of sulfur cycling and $\delta^{34}\text{S}$ fractionation. *Geochim. Cosmochim. Acta* **2014**, *124*, 366–393.
- (42) Sigman, D. M.; Casciotti, K. L.; Andreani, M.; Barford, C.; Galanter, M.; Böhlke, J. K. A bacterial method for the nitrogen isotopic analysis of nitrate in seawater and freshwater. *Anal. Chem.* **2001**, *73*, 4145–4153.
- (43) Casciotti, K. L.; Sigman, D. M.; Hastings, M. G.; Böhlke, J. K.; Hilker, A. Measurement of the oxygen isotopic composition of nitrate in seawater and freshwater using the denitrifier method. *Anal. Chem.* **2002**, *74*, 4905–4912.
- (44) Maher, K.; Bargar, J. R.; Brown, G. E., Jr. Environmental speciation of actinides. *Inorg. Chem.* **2013**, *52*, 3510–3532.

- (45) Fox, P. M.; Davis, J. A.; Zachara, J. M. The effect of calcium on aqueous uranium(VI) speciation and adsorption to ferrihydrite and quartz. *Geochim. Cosmochim. Acta* **2006**, *70*, 1379–1387.
- (46) Bernhard, G.; Geipel, G.; Reich, T.; Brendler, V.; Amayri, S.; Nitsche, H. Uranyl(VI) carbonate complex formation: Validation of the $\text{Ca}_2\text{UO}_2(\text{CO}_3)_3(\text{aq})$ species. *Radiochim. Acta* **2001**, *89*, 511.
- (47) Hsi, C.; Langmuir, D. Adsorption of uranyl onto ferric oxyhydroxides - Application of the surface complexation site-binding model. *Geochim. Cosmochim. Acta* **1985**, *49*, 1931–1941.
- (48) Waite, T. D.; Davis, J. A.; Payne, T. E.; Waychunas, G. A.; Xu, N. Uranium(VI) adsorption to ferrihydrite - Application of a surface complexation model. *Geochim. Cosmochim. Acta* **1994**, *58*, 5465–5478.
- (49) Lieser, K. H.; Thybusch, B. Sorption of uranyl ions on hydrous titanium-dioxide. *Fresenius' Z. Anal. Chem.* **1988**, *332*, 351–357.
- (50) Davis, J. A.; Meece, D. E.; Kohler, M.; Curtis, G. P. Approaches to surface complexation modeling of Uranium(VI) adsorption on aquifer sediments. *Geochim. Cosmochim. Acta* **2004**, *68*, 3621–3641.
- (51) Qafoku, N. P.; Icenhower, J. P. Interactions of aqueous U(VI) with soil minerals in slightly alkaline natural systems. *Rev. Environ. Sci. Bio/Technol.* **2008**, *7*, 355–380.
- (52) Long, P. E.; Williams, K. H.; Davis, J. A.; Fox, P. M.; Wilkins, M. J.; Yabusaki, S. B.; Fang, Y.; Waichler, S. R.; Berman, E. S. F.; Gupta, M.; et al. Bicarbonate impact on U(VI) bioreduction in a shallow alluvial aquifer. *Geochim. Cosmochim. Acta* **2015**, *150*, 106–124.
- (53) Ulrich, K.-U.; Veeramani, H.; Bernier-Latmani, R.; Giammar, D. E. Speciation-dependent kinetics of uranium(VI) bioreduction. *Geomicrobiol. J.* **2011**, *28*, 396–409.
- (54) McMahon, P. B.; Chapelle, F. H. Redox processes and water quality of selected principal aquifer systems. *Groundwater* **2008**, *46*, 259–271.
- (55) Bethke, C. M.; Sanford, R. A.; Kirk, M. F.; Jin, Q.; Flynn, T. M. The thermodynamic ladder in geomicrobiology. *Am. J. Sci.* **2011**, *311*, 183–210.
- (56) Böttcher, J.; Strebel, O.; Voerkelius, S.; Schmidt, H. L. Using isotope fractionation of nitrate-nitrogen and nitrate-oxygen for evaluation of microbial denitrification in a sandy aquifer. *J. Hydrol.* **1990**, *114*, 413–424.
- (57) Aravena, R.; Evans, M. L.; Cherry, J. A. Stable isotopes of oxygen and nitrogen in source identification of nitrate from septic systems. *Groundwater* **1993**, *31*, 180–186.
- (58) Mengis, M.; Schif, S. L.; Harris, M.; English, M. C.; Aravena, R.; Elgood, R. J.; MacLean, A. Multiple geochemical and isotopic approaches for assessing ground water NO_3^- elimination in a riparian zone. *Groundwater* **1999**, *37*, 448–457.
- (59) Cey, E. E.; Rudolph, D. L.; Aravena, R.; Parkin, G. Role of the riparian zone in controlling the distribution and fate of agricultural nitrogen near a small stream in Southern Ontario. *J. Contam. Hydrol.* **1999**, *37*, 45–67.
- (60) Lehmann, M. F.; Reichert, P.; Bernasconi, S. M.; Barbieri, A.; McKenzie, J. A. Modelling nitrogen and oxygen isotope fractionation during denitrification in a lacustrine redox-transition zone. *Geochim. Cosmochim. Acta* **2003**, *67*, 2529–2542.
- (61) Fukada, T.; Hiscock, K. M.; Dennis, P. F.; Grischek, T. A dual isotope approach to identify denitrification in groundwater at a river-bank infiltration site. *Water Res.* **2003**, *37*, 3070–3078.
- (62) Stumm, W.; Morgan, J. J. *Aquatic Chemistry: Chemical Equilibria and Rates in Natural Waters*, 3rd ed.; John Wiley & Sons: New York, 2012.
- (63) Ginder-Vogel, M.; Fendorf, S. Biogeochemical uranium redox transformations: Potential oxidants of uraninite. In *Developments in Earth and Environmental Sciences*; Barnett, M. O., Kent, D. B., Eds.: Elsevier: Amsterdam, 2007; Vol. 7, pp 293–319.
- (64) Abe, Y.; Hunkeler, D. Does the Rayleigh equation apply to evaluate field isotope data in contaminant hydrogeology? *Environ. Sci. Technol.* **2006**, *40*, 1588–1596.
- (65) Clark, S. K.; Johnson, T. M. Effective isotopic fractionation factors for solute removal by reactive sediments: A laboratory microcosm and slurry study. *Environ. Sci. Technol.* **2008**, *42*, 7850–7855.
- (66) Berna, E. C.; Johnson, T. M.; Makdisi, R. S.; Basu, A. Cr stable isotopes as indicators of Cr(VI) reduction in groundwater: A detailed time-series study of a point-source plume. *Environ. Sci. Technol.* **2010**, *44*, 1043–1048.
- (67) Brennecke, G. A.; Wasylenki, L. E.; Bargar, J. R.; Weyer, S.; Anbar, A. D. Uranium isotope fractionation during adsorption to Mn-oxyhydroxides. *Environ. Sci. Technol.* **2011**, *45*, 1370–1375.
- (68) DePaolo, D. J.; Lee, V. E.; Christensen, J. N.; Maher, K. Uranium comminution ages: Sediment transport an deposition time scales. *C. R. Geosci.* **2012**, *344*, 678–687.
- (69) Lee, V. E.; DePaolo, D. J.; Christensen, J. N. Uranium-series comminution ages of continental sediments: Case study of a Pleistocene alluvial fan. *Earth. Planet. Sci. Lett.* **2010**, *296*, 244–254.
- (70) Tricca, A.; Wasserburg, G. J.; Porcelli, D. The transport of U- and Th-series nuclides in a sandy unconfined aquifer. *Geochim. Cosmochim. Acta* **2001**, *65*, 1187–1210.
- (71) Reynolds, B. C.; Wasserburg, G. J. The transport of U- and Th-series nuclides in sandy confined aquifers. *Geochim. Cosmochim. Acta* **2003**, *67*, 1955–1972.